# A MODEL FOR SIMULATION OF FLIGHT PASSAGES THROUGH TRAILING TIP VORTICES

**Yngve C-J. Sedin, Ingemar Gråsjö, Erik Kullberg, Roger Larsson**
***Saab Aerospace***
**S-581 88, Linköping, Sweden (email:** *yngve.sedin@saab.se***)**

**Keywords**: *Vortex wake, aerodynamic model, real time simulation, flight dynamics*

## Abstract

*A model for simulation of flight in a vortex wake behind an aircraft is developed. An interference box is wrapped around the wake. Inside the box incremental aerodynamic forces are computed in a grid as function of position and attitude of the incoming aircraft. The large number of data points required in the aero database called for a linear panel method to estimate the incremental forces and moments induced by the wake. The wake is represented by two rolled up wake vortices with viscous cores. The additional database is superimposed on top of the ordinary. The model was tested in desktop simulations and then implemented in real time simulations with pilot and active flight control system. Results are encouraging. The dynamic response of a fighter was found to be very realistic compared to similar flight tests.*

## 1 Introduction

Flight through trailing wing vortex wakes is by no means a new experience. This has occurred since the WW-I time when pilots encountered vortex wakes trailing from maneuvering aircraft or sometimes even flew into their own wakes.

Today, for several reasons, the subject is of greater importance. With increasing air traffic around airports and in flight corridors, there are safety aspects, see e.g. in Ref [1], ranging from dynamic flight behavior to concern about structural loads or time separation during take-off and landing. Modern fighters with relaxed static stability are also extensively relying on active flight control systems. This trend is seen also with modern civil aircraft. All this together has given new dimensions to the problem.

Flight control systems are processing information from sensors like accelerometers, weather vanes and pressure gauges. On this information the system is responding. The pilot is acting, interacting and reacting in this scenario. How this will take place in wake encounters and what response there will be is not easy to tell. Simulation models are required.

The wake consists of quite complex mixed flows. In simplified terms the strength of end tip vortices is proportional to the weight and the load factor but inversely proportional to the wingspan and the speed of the generating aircraft. Vortex core diameters are usually just fractions of the wingspan. The region of induced interaction away from the cores is of the order of the wingspan. The core vorticity is decaying slowly while the core diameter is growing downstream. The vortex circulation can persist for several minutes or several tenths of miles behind the shedding aircraft in still air.

Methods for simulation of wake encounter in six degrees of freedom have been rare. The present project was set the aim of going from model development to demonstration of simulations within one year. Results are encouraging. Simulations have indicated good similarities with flight tests performed with a similar type of aircraft as addressed here. Presentations have been made at conferences in Moscow [2] and in Söderköping [3]. The present paper is presenting background and details of the model together with some results.

## 2 General

### 2.1 Background

All aircraft ('A/C') will react some way or the other on interacting vortical flow encountered in vortex wakes. The dynamic response will depend on the generating A/C, the incoming A/C itself and the speed and flight path taken through the wake.

Since long, there has been an interest both from the Swedish Defense Material Administration (FMV) and from Saab to make flight tests of aircraft flying through end tip vortices. The SAAB 37 Viggen was extensively tested using the same type of lead aircraft provided with a smoke aggregate for visualization. Violent disturbances in roll could be obtained as well as short times of afterburner flameouts. Shallow wake interception angles gave exposure times for pronounced motion responses. More open angles could presumably excite structural eigen-mode frequencies.

During the 1970's one incident is known when the upper part of the vertical fin of a SAAB 37 Viggen was lost due to a likely wake encounter. This was verified later by aeroelastic analysis. In 1999 another incident occurred when a SAAB 39 Gripen was lost in connection with vortex wake encounter practicing air combat below 3000 ft. In 2001 an Airbus A300 got its fin ripped off in a likely wake encounter.

During 1999 the subject was seriously raised of developing a model for dynamic analysis and real time simulation of flight through wake vortices. Project requirements were set for going from development to demonstration within one year of work. In this perspective, considering the complexity, generic simplicity had to be of leading concern using existing software and simulation facilities when possible. The work was undertaken during year 2000 and finished in early 2001.

### 2.2 Model Requirements

Requirements were set as follow for developing a real time simulation model:

- Development time within one year
- Desktop and real time simulation in six degrees of freedom (translation-rotation)
- Generic simple model Fig 1 of vortex wake behind generating A/C (G).
- Incoming A/C (B) to enter wake zone at any position and attitude with course and speed different from G, see Fig 1.
- Buildup of incremental aero database for B within reasonable computing time.
- Rapid method for estimating incremental forces and moments on B (Fig 1).
- Rapid method for estimating local flow direction increments at vane positions.
- Easy plug in of other types of aircraft A and B for simulation.
- Existing technique for model calibration of incremental aero database.
- Same databases and software in both desktop and real time simulations.

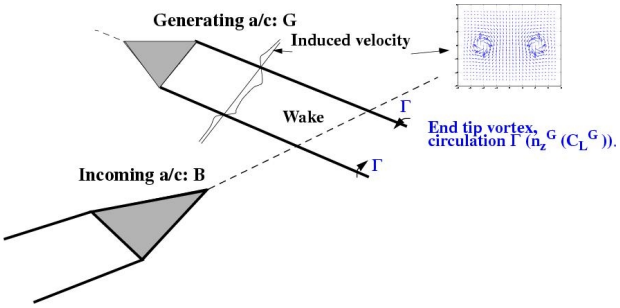


**Figure 1. Generic concept of wake passage**

To carry on the concept of Fig 1, the following elements were needed:

1. Viscous wake model of generating aircraft G.
2. Model to estimate incremental forces induced by wake on B.
3. Method to estimate incremental flow angles at weather vanes of B.
4. Incremental aero database arranged in look-up tables for incoming B.

It was assumed that the aero database in element no. 4 above should be computed in advance. Moreover, the method for computing the incremental forces and moments in no 2 as

well as flow directions at vane positions, no 3, should be fast to generate a whole database in space around the wake. Recalling that classic linear and non-linear potential flow is executed on computers within seconds or minutes and the more advanced non-linear flow models, as Euler or Navier-Stokes, require hours or days for just one flight case, the choice of flow model became fairly obvious.

## 2.3 Model: Idea and structure

Inventing different possibilities finally led to the following model traced down in part models

- *Aerodynamic model*
- *Aero database model*
- *Simulation model*

The *Aerodynamic model* consists of both the wake flow model behind the generating A/C named G as well as the computational model for estimating incremental forces and moments induced by the wake on the incoming A/C named B, for notations see in Fig 1.

The *Aero database model* consists of digital look-up tables for aerodynamic forces and moments. It was here completed with incremental forces and moments due to the wake influence. An interpolation routine is calling incremental data as function of B's position B(x, y, z) and angular Euler attitude B($\phi$, $\theta$,$\psi$) inside an interference box surrounding the wake, see in Fig11. The orientation and location of the incoming B is relative to the generating G's coordinate system.

With *Simulation model* is here meant the software and database installations for flight control and time integration of the equations of motion. There are two optional simulation facilities, the desktop operated 'ARES' and the real time simulator 'STYRSIM'. Simulations can be performed either in desktop mode or in real time with pilot, active flight control system and an outer world environment. Both simulators are using the same software and databases.

In summary, the bearing idea generally was to create an incremental database of aerodynamic forces and moments induced by the presence of the wake. This was to be used by superposition on the ordinary database valid in homogeneous atmosphere. The latter includes all static aerodynamic coefficients, control surface coefficients and dynamic derivatives. The increments due to the presence of the wake were to be theoretically computed as function of position and attitude inside an interference box only. Influences on rudder effectiveness or damp derivatives due to the wake were not considered. They all stayed the same as in the corresponding database for homogenous air.

With this overall model approach, simulations could be taken on relatively easy. It should be noticed that the incremental database became about five times the volume of the conventional database in homogenous air. Hence, enough memory space must be available.

## 2.4 Software for build-up of aero database

The program system Ref [4] for build up of the incremental aero database is shown in the block chart Fig 2 below:

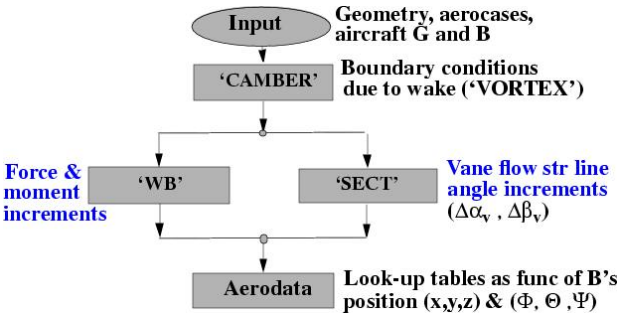


**Figure 2. Program system for aero database**

In 'Input' the involved aircraft and requested aero cases are defined. The module 'CAMBER' is setting up equivalent camber slopes serving as local boundary conditions on B, see Figs 1, 3. It is calling the subroutine 'VORTEX' (not shown in Fig 2) for calculating the local wake velocities induced by the two

trailing end vortices together with the bound vortex representing the wing load of aircraft G.

The linear panel code 'WB' is for computing incremental forces and moments, while 'SECT' is a 2D cross-flow panel code for estimating incremental flow direction inclinations at vane positions in fuselage sections, Figs 3-4,10.

Once the input for G and B is established and the aerodynamic influence coefficient matrix in 'WB' is computed, calculation of one data point of the aero database takes about 1 CPU second. The number of panels is about 500. The computer is an SGI Octane with one 195 MHz R10000 processor.

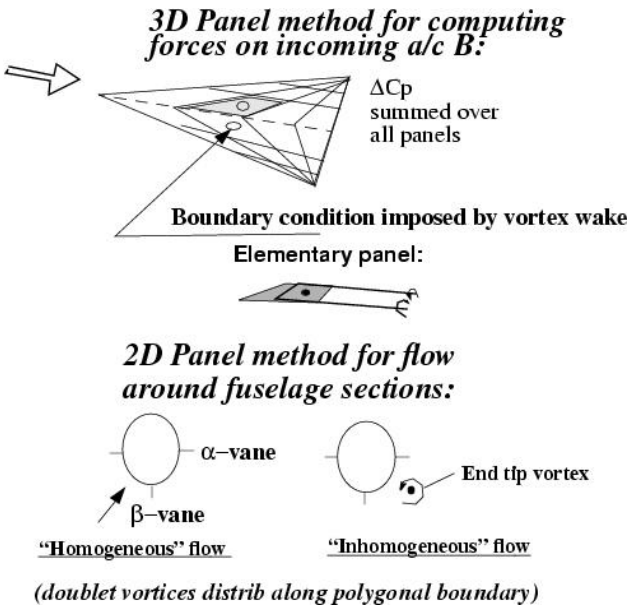


**Figure 3. Panel methods and generic models**


**Figure 4. SAAB 39 Gripen with reference positions of weather vanes and center of gravity (CG) indicated**

## 3 Aerodynamic Model

### 3.1 Wake model

The wake model consists of two end vortices with viscous cores separated by a distance equal to the span b of G. For simplicity the vortices are assumed to be straight and aligned with the speed of the generating aircraft G, see in Fig 5.

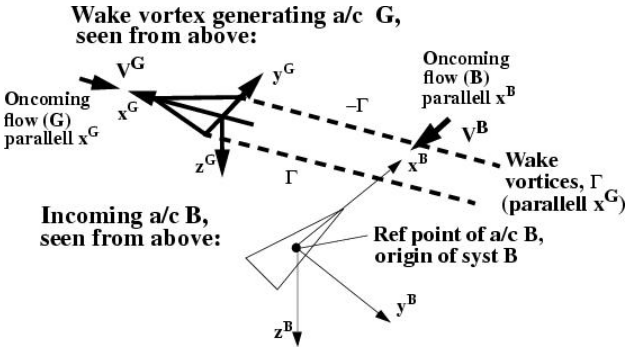


**Figure 5. Wake and coordinate systems.**

No interference from the incoming B onto the wake is considered. Aircraft G has no more geometric details than the span $b$ and the reference area $S$. The operating conditions are primarily given by the mass, the normal g-load factor, and the flight Mach number $M^G$ and the flight altitude of A/C G. With this, the lift coefficient $C_L$ and the speed $V^G$ can be derived for G in order to estimate the wake vortex circulation $\Gamma$, see in Fig 6.

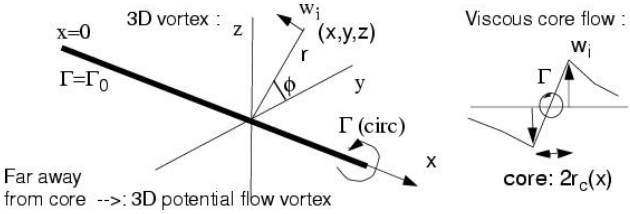


**Figure 6. Wake trailing tip vortex.**

The tip vortex, illustrated in Fig 6, is trailing downstream, while its strength is assumed to be exponentially decaying with x behind aircraft G.

$$\Gamma(x) = \Gamma_0 e^{-D \cdot x}, \quad \Gamma_0 = \frac{S}{2b} V^G C_L \qquad (1)$$

The frame *(x, y,z)* in Fig 6 is following with G. Two types of vortex cores were considered.

*3.1.1 Vortex with the Lamb velocity profile*

Using the local coordinate system of Fig 6 with x pointing downstream and the origin at the end of aircraft G, the induced circumferential velocity $w_i$ is modeled as a viscid-inviscid 3D compound expression with the 'Lamb' core velocity profile as follows

$$w_i = \frac{\Gamma}{4\pi \cdot r}\left(1-e^{-\theta}\right)\left(\frac{x}{\left(x^2+\beta^2 r^2\right)^{1/2}}+1\right) \qquad (2)$$

$$\theta = \theta_c \cdot \left(\frac{r}{r_c}\right)^2, \quad r^2 = y^2 + z^2 ,$$

$$\beta^2 = 1-\left(M^G\right)^2$$

$r_c$ denotes the vortex core radius. The constant $\theta_c$ is equal to 1.2565. The core radius $r_c$ is growing downstream and it is expressed by the formula

$$r_c^2 = r_{c,0}^2\left(1+4\frac{\theta_c}{\mathrm{Re}_{c,0}}\cdot\frac{x}{r_{c,0}}\right) \qquad (3)$$

The initial vortex core radius at x= 0 is assumed to be

$$r_{c,0} = \frac{c_1}{4\cdot\pi}\left(1-e^{-\theta_c}\right)\frac{b}{A} \qquad (4)$$

A is the wing aspect ratio of the generating aircraft and $c_1$ is an available constant, in present simulations set to 1.42857. The core Reynolds number and the effective viscosity ansatz have the expressions

$$\mathrm{Re}_{c,0} = V^G \cdot r_{c,0}/\nu_e \qquad (5)$$

$$\nu_e = \nu\left(1+\frac{c_2}{(2\pi)^2\theta_c}\cdot\frac{\Gamma}{\nu}\right) \qquad (6)$$

$\nu$ is the kinematic viscosity and $\nu_e$ is an 'effective' kinematic viscosity. $c_2$ is another available coefficient, here set to 0.0016. The decay coefficient of the circulation is written

$$D = \frac{c_3 \cdot Tu}{V^G b} \qquad (7)$$

$c_3$ is still another calibration coefficient, here set to 0.8. Tu is a typical turbulent velocity fluctuation in the surrounding air and $V^G$ is the speed of aircraft G through the atmosphere.

The appearance of Eq (2) is such that at large distances from the core it behaves similar to a half-infinite 3D potential flow vortex, except for the extra ageing decay according to Eq (1). Closer to the core it is similar to a 2D potential vortex. Very close it is analogue to an exact 2D viscous Navier-Stokes solution of a vorticity decay problem (see e.g. Ref [5]), where the real time is substituted by $x/V^G$. In fact, this solution was also achieved by linearising the steady 3D Navier-Stokes equations shown in Ref [6]. The model structure as described by Eq (2) was developed and suggested in Ref [7] for weapons separation and chaff release studies in the early 1990's.

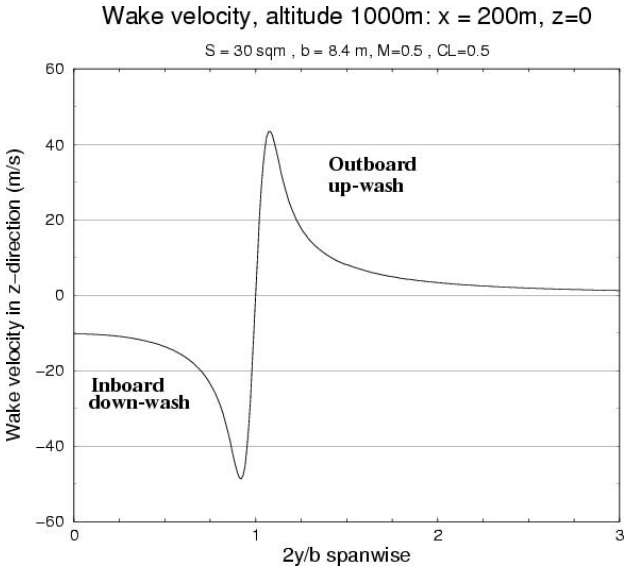


**Figure 7. Typical wake induced velocity**

The total induced wake flow is set up by contributions from the 'bound' parts of the horse shoe vortex representing lift on G plus the

two trailing viscous vortices as described by Eq(2). One example (G as in Figs 4, 9) on combined wake flow with contributions from trailing and bound vortices at constant x is shown in Fig 7. The wake model can partly be calibrated by tuning available constants $c_1$, $c_2$ and $c_3$.

*3.1.1 Vortex with expanded Lamb profile*

Normalizing the rotational velocity distribution by the maximum, see Fig 8,

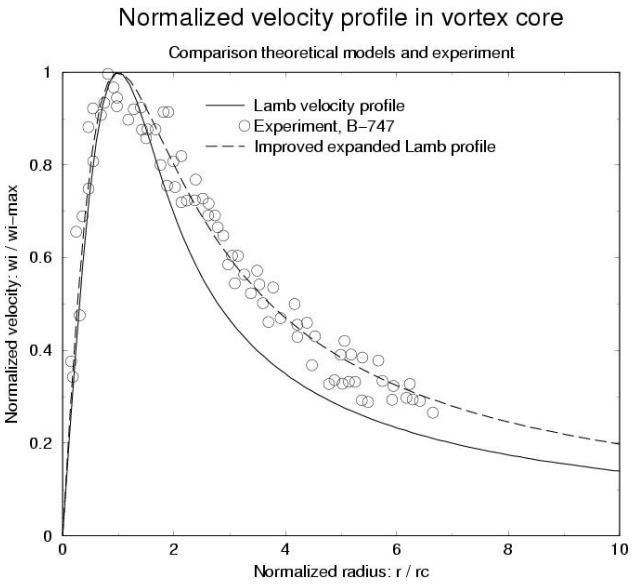


**Figure 8. Self-similar vortex core profiles**

it turned out that the Lamb type profile Eq (2) gave too narrow a peak region and that the core circulation seemed too high compared to experiment, Ref [8].

A new model was then created by expanding the viscous part of Eq(2) with regard to small θ forming a rational expression with nominator and denominator linear in θ:

$$w_i = \frac{\Gamma}{4\pi \cdot r} \cdot \frac{\theta}{1+\theta} \cdot \left( \frac{x}{\left(x^2 + \beta^2 r^2\right)^{1/2}} + 1 \right) \qquad (7)$$

The asymptotic far field behavior of Eq(7) is still the same as with the Lamb profile Eq(2). However, the inner region is different and the peak core velocity appears at the core radius $r_c'$ slightly smaller than that of Lamb's. Renormalization of Eq (7) then leads to Eq (8) as follows

$$w_i = \frac{\Gamma}{4\pi \cdot r} \cdot \frac{\theta'}{1+\theta'} \cdot \left( \frac{x}{\left(x^2 + \beta^2 r^2\right)^{1/2}} + 1 \right) \qquad (8)$$

$$\theta' = \left( \frac{r}{r_c'} \right)^2 , \quad r_c' = \theta_c^{-1/2} \cdot r_c ,$$

$r_c$ is as in Eq (3). Quite an improvement is found in Fig 8 in favor of results from Eq(8) when compared to data from Eq(2) and experiments, Ref [8].

### 3.2 **Force and vane flow models**

The model for estimating incremental forces and moments induced by the wake is based on linear potential theory as sketched in Fig 3. The panel method for computing the overall configuration of incoming B is similar to that of Ref [9]. The panel model of the SAAB 39 Gripen fighter is shown in Fig 9 below

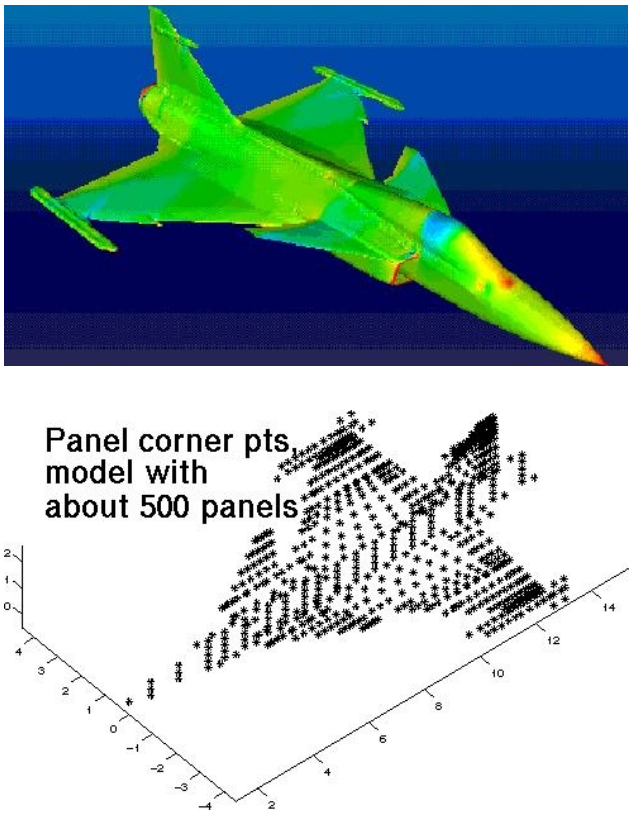


**Figure 9. Panel model of incoming aircraft B**

The panel method for estimating induced streamline inclinations at weather vane positions in fuselage sections (Figs 3-4,10) was developed solely for this task. It consists of 2D doublet panels with contra rotating elementary vortices at ends of panels. Cross-flow boundary conditions are created at all panels mid points by the imposed wake flow. The local tangential cross-flow was derived at panel corner points by smearing the local resulting corner circulation over the corresponding neighboring arc lengths. This method gave good enough agreement with wind tunnel measured streamline inclinations in uniform flow. The fuselage sections are as shown below

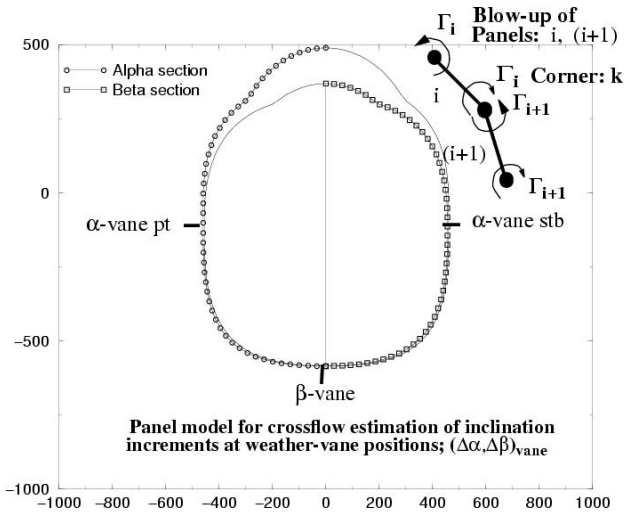


**Figure 10. Fuselage α/β-vane cross-sections.**

For both panel methods, let $\mathbf{w}^B_i$ be the induced wake velocity in any control point i of a panel and let $\mathbf{n}^B_i$ be the corresponding out-leading surface normal in that same point. The imposed normal velocity $v_n{}^B_i$, exerted by the wake on panel control point i, is defined by the scalar product

$$(v_n)_i^B = n_i^B \circ w_i^B \qquad (8)$$

Let $A_{ij}$ be the influence coefficient matrix in the 3D panel program 'WB' (Figs2,3) inducing normal velocities by panel singularities $\Gamma^B_j$ in panel control points i. The boundary condition solving all singularities $\Gamma^B_j$ then comes out by annihilating the imposed normal velocities as follows

$$\sum_j A_{ij}\Gamma^B{}_j + (v_n)_i^B = 0 \qquad (9)$$

The normal velocities Eq (8) are in 3D transferred into camber slopes in the module 'CAMBER' (Fig 2). The slopes are input to the panel program 'WB' (Fig 2) for solving Eq (9). Forces and moments on B are calculated from the bound vortex singularities $\Gamma^B_j$.

A similar path is taken with the 2D cross-flow panel method 'SECT' (Figs 2, 3) for solving streamline inclinations due to the wake in vane positions (Fig10). Let $C_{ij}$ be the influence coefficient matrix of the vortex doublet panels with vortices $\Gamma^B_j$ in the considered cross section. Assume $v_n{}^B_i$ to be the normal velocity imposed by the wake in panel control point number i. The vortex doublets solutions $\Gamma^B_j$ are solved from the following system of equations by annihilating $v_n{}^B_i$

$$\sum_j C_{ij}\Gamma^B{}_j + (v_n)_i^B = 0 \qquad (10)$$

A non-singular diagonal dominance of $C_{ij}$ is artificially numerically secured inside 'SECT'. For evaluation of the tangential velocity $v_t{}^B_k$ in corner point k between neighboring panels i and i+1, let the panel lengths be $s_i$ and $s_{i+1}$. A numerical estimate at corner k of the tangential velocity $v_t{}^B_k$ then comes out along the section contour including the wake contribution:

$$(v_t)_k^B = \frac{\left(\Gamma_{i+1}^B - \Gamma_i^B\right)}{\left(s_{i+1} + s_i\right)} + t_k^B \circ \frac{\left(w_i^B + w_{i+1}^B\right)}{2} \qquad (11)$$

$\mathbf{t}^B_k$ is the tangential unit vector along the arc length at corner k. Notations $\mathbf{w}^B_i$ and $\mathbf{w}^B_{i+1}$ are here the summed up velocities in control points i and i+1 coming from the wake and all vortex doublets.

With Eq (11), changes in streamline inclinations due to the wake can be calculated at vane positions. In uniform flow numerical tests gave the computed angle of attack gradient $d\alpha_{vane}/d\alpha$=1.66, while experiments in a wind

tunnel for the same A/C B (Fig 4) gave the local angle of attack change $d\alpha_{vane}/d\alpha=1.61$. A similar evaluation for sideslip gave $d\beta_{vane}/d\beta=1.72$ and in the wind tunnel the value $d\beta_{vane}/d\beta=1.65$ was obtained. This accuracy was accepted for simulation studies.

## 4 Incremental Aero Database Model

Incremental aerodynamic forces and moments and local streamline angles at vane positions on the incoming B are computed inside an interference box wrapped around the wake. Data is stored in grid nodes of system $(x^G,y^G,z^G)$ following the generating A/C G, see in Fig 11.

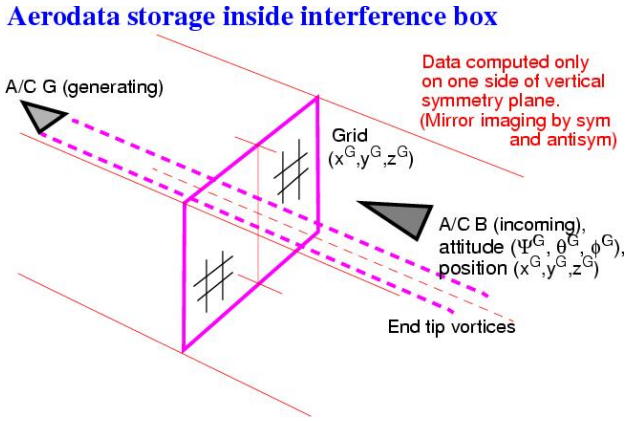


**Figure 11. Interference box for data storage**

Three incremental forces and moments (Fig 12) and three streamline inclinations at vane positions (Figs 4, 10) are computed for the incoming A/C B in a quasi-steady manner.

The quasi-steady approach was first checked against unsteady aerodynamic results obtained by a linear flutter program, Ref [10], using the wake as a complex wind gust. The wake passage was prescribed and the time history of forces and moments were injected into simplified dynamic simulations with ordinary damp derivatives added. It was found that the differences in time history of the Euler angles were small compared to the quasi-steady approach for shortly endured simulation times. Hence, the quasi-steady model (Figs 1,3,5) was chosen. This is in agreement with how the ordinary aero database is set up for simulations.

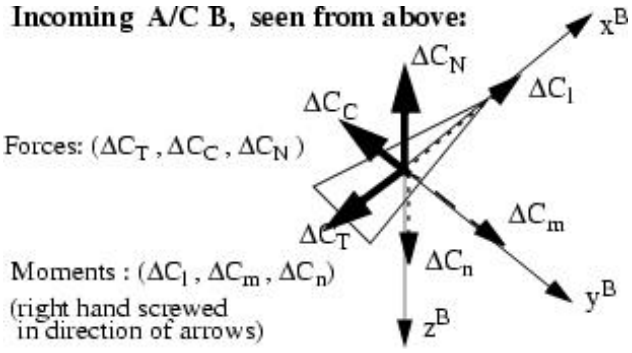


**Figure 12. Forces and moments due to wake**

Increments in forces $(\Delta C_T, \Delta C_C, \Delta C_N)^B$ and moments $(\Delta C_l, \Delta C_m, \Delta C_n)^B$ as well as vane streamline angles $(\Delta\alpha_{vstb}, \Delta\alpha_{vpt}, \Delta\beta_v)^B$ for flight control are considered in computations. There are two α-vanes for starboard and port sides respectively, but only one β-vane, see in Fig (10). There are nine primary variables to calculate for every reference position $B(x^G,y^G,z^G)_i$ and Euler attitude $B(\phi^G,\theta^G,\psi^G)_k$ relative to G, see partly in Figs 4-5 and 11-12. This means nine main variables as function of six degrees of freedom organized in a look-up table for fast real time interpolation during simulations. Symbolically the total aerodynamic database on coefficient form is established by superposition:

$$C^B_{x,total} = C^B_x + \Delta C^B_x\left(x^G, y^G, z^G, \phi^G, \theta^G, \psi^G\right) \qquad (12)$$

$C_x^B$ above is representing the ordinary database in uniform air and includes all control surface effects, that are kept the same, as well as all the damp derivatives for dynamic simulations.

The incremental database is almost one order of magnitude larger than the ordinary in uniform air. To save storage and computing time the right hand side of the interference box needs to be considered only due to symmetry and anti-symmetry. To simplify further, only one cross section grid plane (Fig 11) was calculated. Based on sparse numerical calculations, the x-dependence was functionally extended outside that cross-section plane in

order to cover the event of space. The wake interference database can be scaled regarding changes in the speeds of G and B as well as of changes in the load factor of G.

Typically 323 node locations $B(x^G,y^G,z^G)$ were used for constant $x^G$ (see Figs 5, 11), in combination with (7,7,5) values of Euler attitude angles $B(\phi^G,\theta^G,\psi^G)$ in every node. This means about 700 000 function values in one constant $x^G$-plane with data analytically continued for decreasing and increasing values of $x^G$ outside the chosen cross reference plane.

## 5 Simulation Facilities and Model

Two different facilities have been considered in simulations. Both are using the same type of software and databases. One is named ARES that is for dynamic desktop simulations. The other called STYRSIM is for real time simulations with pilot and active flight control system. ARES is a desktop available simulator for development and testing of flight control laws as well as for replaying recorded flight tests. STYRSIM is for real time simulations, development and testing of control laws with a pilot-in-the- loop. It is also used for flight test preparations. STYRSIM has got an in-house developed outer world environment and a simplified internal cockpit environment. The data sampling frequency is 120 Hz. The ordinary aero database in uniform air was supplemented with an incremental database due to the wake in accordance with Eq(12).

Rapid linear multi-variable interpolation algorithms were used for calling the nine primary functions in the additional database within the space of six degrees of freedom, B $(x^G,y^G,z^G)$ and B $(\phi^G,\theta^G,\psi^G)$. The position and Euler attitudes are all expressed relative to G. Fig 13 is showing real time simulations in the STYRSIM simulator. The cockpit is provided with control stick, foot pedals and throttle lever and some instrumentation.

In the upper part of Fig 13 the cockpit is shown from behind with the pilot banking to the right. The white and red bands located at ten o'clock in the upper figure are markers for the rolled up vortex cores. In the lower part of Fig 13 the pilot is banking to the left and the vortex markers are seen at two o'clock. Pictures in Fig 13 were extracted from the video recording in Ref [11].

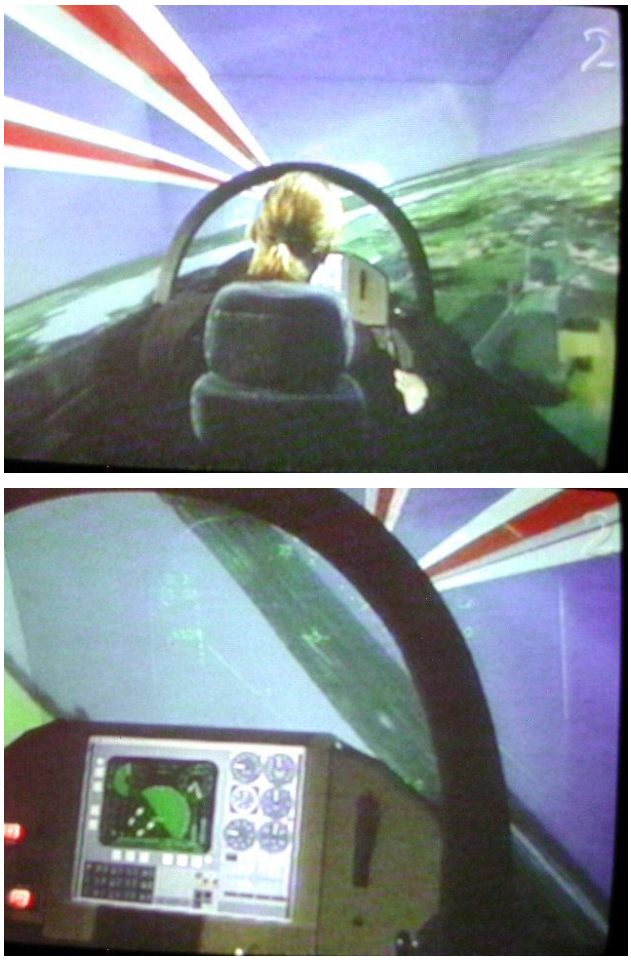

**Figure 13 Simulation of wake encounter.**

## 6 Results

### 6.1 Traversing the wake

An impression of wake induced forces and moments (Fig 12) traversing the wake can be seen in Figs 14-15. Aircraft B (see Figs 9, 5) is moved through the wake region by translation laterally 1 m above the vortex cores and $x^B$ in parallel with $x^G$. The translation is performed 200 m behind the generating aircraft G that is of the same type as B. The span is b=8.4 m and the reference area S=30 $m^2$ of both. The operating lift coefficient of G is $C_L$ = 0.2 and the Mach number about M=0.5 of both. Local disturbances on the graphs (Fig 14) of induced

tangential and side forces respectively are clearly observed when any of B's wing tips or fuselage is passing above any of the vortex cores. An interesting notation is that the induced normal force on B is fully recovered from G with negative sign when the CG reference position of B is in the middle between the two wake vortices. Hence, Newton's law of action and reaction is fulfilled a fact being recognized also in real flight tests.

Fig 15 is showing the wake induced aerodynamic moments (see Fig 12). The pitching moment is symmetric while the lateral coefficients are asymmetric, as they should. The local extremum behavior of the pitching moment located in between the end tip vortices are due to the smaller downwash obtained there compared to the immediate surrounding, see e.g. the downwash in Fig 7.

In Fig 16 induced streamline inclinations are illustrated in three vane positions, see Figs 4,10. The port and starboard $\alpha$-vane positions show slightly asymmetric inclination values as they should due to the width of the fuselage in that section, (Fig 10). The $\beta$-vane position is showing an asymmetric behavior with strong local peak values when passing over the vortex cores.

### 6.2 Desktop simulation

A time history impression of the motion pattern in terms of aircraft B's attitudes from a desktop simulation in a shallow wake interception is shown in Fig 16. The Mach number is M=0.5 and the event takes place at 200 m behind the leading aircraft. Six discrete time exposures are marked for the roll, pitch and yaw angles respectively. In Fig 17 snap-shots are taken at indicated times numbered from 1 to 6. The time history is simultaneously recorded in an in-house developed visualization system called 'VISOFLY', Ref [12], working either with a moving external world seen from the cockpit or by showing the aircraft motion externally seen from a frame following B. VISOFLY was originally developed for weapon release simulations and later used for flight test visualizations. Instruments and indicators are simultaneously shown on the monitoring screen.

## 7 Comments and Discussions

### 7.1 Comments on the model

It is believed that the present physical model is good enough for starting serious attempts of simulating aircraft dynamics during wake encounters. Pilots have judged observed visual responses to be realistic. Peak load factors and roll amplitudes are in agreement with those found in flight tests. There are ideas how to handle improvements empirically by calibration and tuning the database inside the interference box, but also how to make further developments in the physical and mathematical models.

One obvious improvement is to integrate curved vortex paths under mutual influence from the generating aircraft and the trailing vortices. In the present study they were straight lines to get development going as quick as possible. Maybe this is not so important 'per ce' for simulations once the wake is encountered. However, when analyzing and adapting data to flight tests this information should be of importance.

There is no influence by the incoming aircraft itself on the path of the trailing vortex wake. Such influences have been seen in flight tests with two SAAB 37 Viggen aircraft. If deemed necessary, further developments of the mathematical model should incorporate these effects.

Concerning the linear panel method, when computing incremental loads, empirical saturation of camber slopes could be one way to go when very high local streamline inclinations occur due to the close vicinity of vortex cores with strong velocities. This would avoid too stiff aerodynamic responses when outside the scope of linear theory. An aero-elastic influence coefficient matrix is optional in the 3D panel method. However, loads due to the wake as presented here were computed with rigid aircraft only, although aero-elastic rudder efficiency degradations are included in the

basic aero database (see in connection with Eq(12)).

The axial vortex core velocity distribution, neglected here, is one item that could be added to the model as well as the core flow from a jet engine or a propeller wake. A maneuvering lead aircraft is another interesting development making the wake even more complex with spiraling vortices. However, due to the complexity and amount of data involved, simplicity still has to be of leading concern in future developments.

### 7.2 On applications

There are several applications where simulation methods are in demand for flying in wake vortices or in the vicinity of trailing vortex wakes.

The simulation model is a tool for development, analysis and checking of flight control laws. Obvious applications are in flight safety investigations, development of procedures for flying in tight formations, energy efficient optimization of formation flying, simulation of air refueling, training and demonstration of wake encounters. Special investigations in simulation of flying in formations with UAVs can be carried on.

Aerodynamic loads for structural analysis are inherently available from the panel method computations when building up the incremental aero database. Hence simulated time histories can be analyzed from a structural point of view.

There is a vast and important field of flight safety issues around congested airports. In that case the physical wake model has to be improved regarding wake dissipation, influence from ground proximity, ground turbulence, wind shear and wind drift. Still however, simplicity must be of leading concern when modeling for real time simulations

## 8 Concluding remarks

A model for desktop and real time flight simulation of vortex wake encounter was developed. Simulations were demonstrated in six degrees of freedom. Effects by the wake on weather vanes were included as well as dynamic modeling of vanes. Aerodynamic loads are inherently available for structural analysis.

The additional aero database became almost one order of magnitude larger than the conventional used for simulation in uniform air. Nine primary variables as function of six degrees of freedom were handled. The database can be scaled with respect to nominal flight conditions.

Although simple, it is believed that the present model has the potential of capturing the main physical elements for meaningful and valuable simulation studies. Achieved results are encouraging. Load factor peak values and roll amplitudes are in surprisingly good agreement with data found in flight tests with similar aircraft.

The model can be used for development of flight control systems; control laws; flight safety investigations as well as for demonstrations of wake encounters. There are possibilities of further theoretical improvements and empirical adaptation of data to flight test results and other experiments.

## Acknowledgement

The authors want to thank the Swedish Defense Material Administration (FMV) for moral and financial support given to this project.

## References

[1] Vyshinski V.V. Flight safety, aircraft vortex wake and crisis of airports. In *Scientific Seminar: Investigation of Vortex Wake Evolution and Flight Safety Problems*. Trudy TsAGI. Vol 2627. Moscow 1997, pp 5-23.

[2] Gråsjö I, Kullberg E, Larsson R, Sedin Y. Flight Mechanical Real Time Simulation of Flight through wake-vortices. Presentation at *Aerospace Technologies of the XXI Century: New Challenges in Aeronautics- Flight Dynamics.* Moscow, Aug 2001.

[3] Kullberg E, Gråsjö I, Larsson R, Sedin Y. Simulation of Flight in Wing Tip Vortex. Presentation at *Society of Flight Test Engineers-EC*, Söderköpings Brunn, Söderköping, Dec 2001.

[4] Sedin Y. C-J. Program system and file structure for linear computation of loads as experienced in passage of end tip vortices- Version No 01. *Internal Saab report (in Swedish). Saab Aerospace, Future Products. Report FTA-2002-0005*. Dated Nov 16, 2000.

[5] Schlichting H. *Boundary layer theory*. McGraw-Hill, 1960, pp 71.

[6] Newman B.G. Flow in a viscous trailing vortex. *The Aeronautical Quarterly*. May 1959, pp149-162.

[7] Sedin Y. C-J. Induced velocities around a 3D end tip vortex with and without viscous core for weapons separation simulations. *Saab internal working reports. Saab Aerospace, Aerodynamics Dept.* 1990-1992.

[8] Burnham D.C, et al. 1978 Ground-Based Measurements of a B-747 Aircraft in Various Configurations. *US. Dept of Transportation Report FAA-RD-78-146.*

[9] Woodward F.A. Analysis and design of wing-body combinations at subsonic and supersonic speeds. *AIAA J. of Aircraft*, Vol. 5 No. 6, Nov-Dec 1968.

[10] Winzell B. Response of the rigid aircraft flying close to end tip vortices. Saab *Aerospace, Gripen. Report GMFL-2000-0050. (Report in Swedish).* May 26, 2000.

[11] TV program NOVA. Program on wake vortices. – *SVT-Swedish Radio & Television, Channel TV2.* April 08, 2002.

[12] Lindberg A. VISOFLY, a flight path visualization program- Version 9.7. *Saab Aerospace, Gripen.* May 11, 1998.

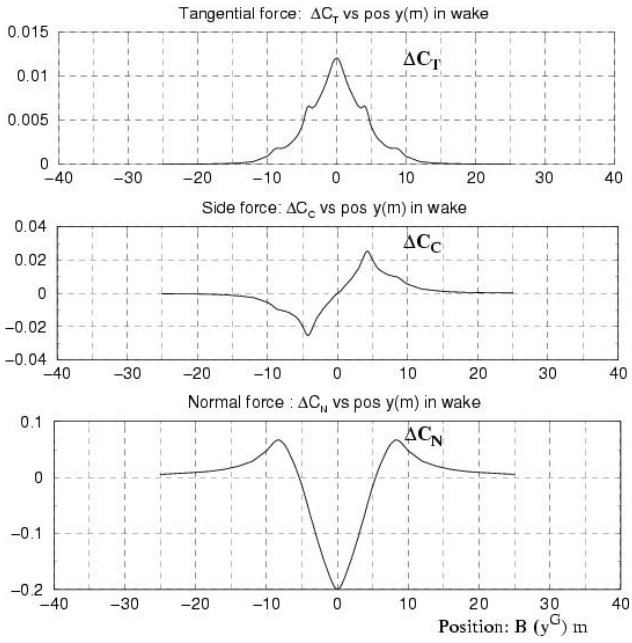


**Figure 14. Induced forces traversing B above vortex cores, 200 m behind generating G**

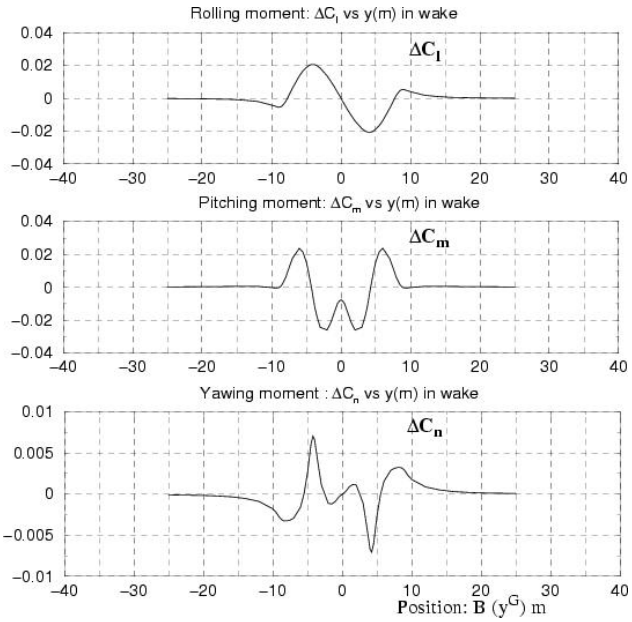


**Figure 15. Induced moments traversing B above vortex cores, 200 m behind aircraft G**

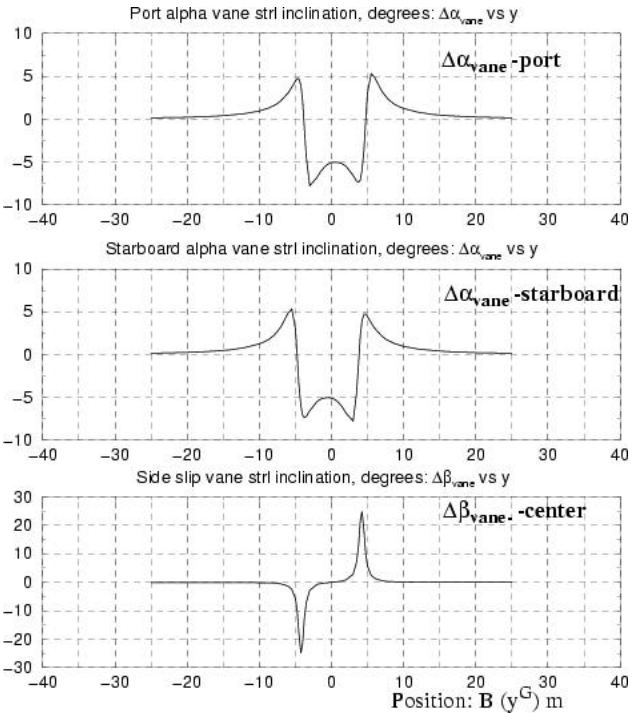


**Figure 16. Induced streamline inclinations at vane positions, traversing B above vortex cores, 200 m behind generating aircraft G**

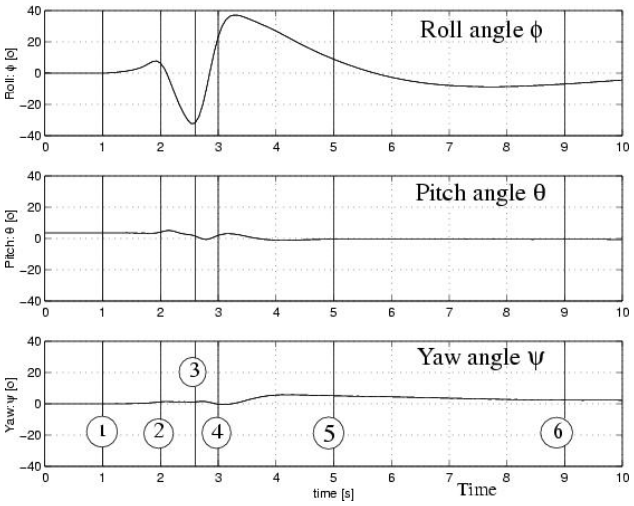


**Figure 17. Desktop simulation of shallow wake interception about 200 m behind aircraft G. Time history of Euler angles $B(\phi,\theta,\psi)^G$ in degrees, time in seconds**

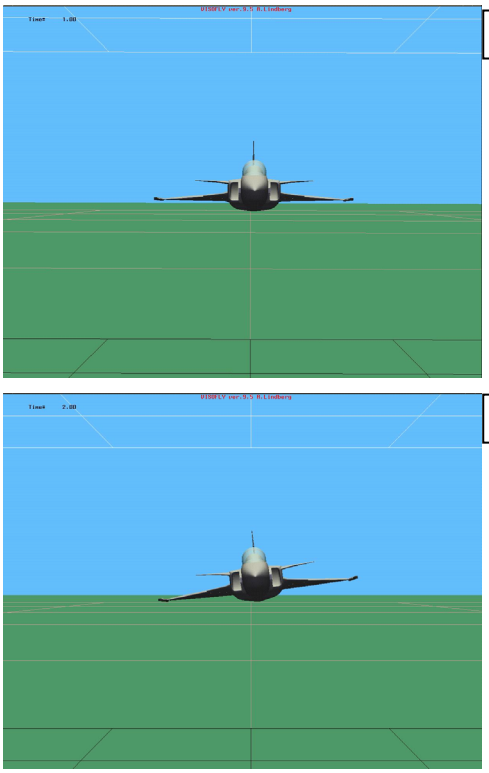


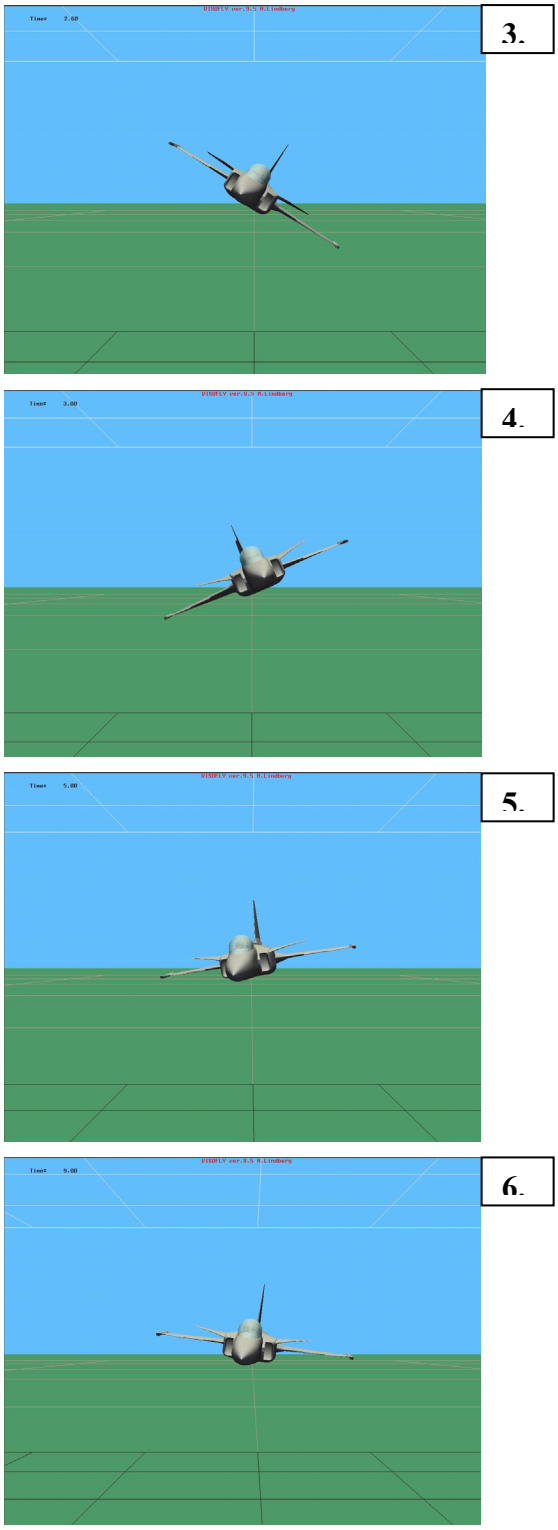


**Figure 18. Sequence of snapshots 1-6 of desktop simulation shown in Fig 17**